Peptide Modeling

Stability of SIV gp32 Fusion-Peptide Single-Layer Protofibrils as Monitored by Molecular-Dynamics Simulations**

*Patricia Soto, Josep Cladera, Alan E. Mark, and Xavier Daura**

Amyloid fibrils are filamentous structures formed from peptides and proteins of widely varied sequence and length.[1,2] Such noncovalent assemblies are at the heart of a wide range of diseases including Alzheimer's and Creutzfeld–Jakob disease (CJD) in humans, and bovine spongiform encephalopathy (BSE) in cattle.[3] These protein-conformational diseases are particularly intriguing, because, given appropriate conditions, the formation of amyloid aggregates appears to be a generic property of constituent polypeptides and is largely independent of their source.[3] The biophysical factors that determine whether specific sequences will form stable amyloid suprastructures are largely unknown. Furthermore, high-resolution structural data has proved difficult to obtain because the fibrils are insoluble and noncrystalline.[1] X-ray diffraction patterns from amyloid fibers are consistent with a cross-β structure.[4] This, in conjunction with information from solid-state NMR spectroscopic analysis,[5] cryoelectron microscopy, and image processing,[6] has led to the proposal of models for amyloid protofilaments that consist of multilayered, helical β sheets. The structural features of the fibrillar forms of different proteins are very similar. This suggests that fibrils form by a common mechanism, and that the elucidation of the assembly process in one system will shed light on amyloid formation in general.[1–3] Herein we report atomistic molecular-dynamics (MD) simulations performed in explicit solvent to investigate the supramolecular organization of a single-layer protofibril formed from the simian immunodeficiency virus wild-type (SIVwt) peptide.

The SIVwt peptide corresponds to the N-terminal region of the SIV transmembrane glycoprotein 32 (gp32) (GVFVLGFLGFLA). It is involved in triggering the fusion of viral and target cell membranes, which facilitates entry of the virus into the cell.[7] This 12-residue peptide is very hydrophobic, a property shared with the Aβ(30–40) C-terminal segment of the amyloid peptide responsible for Alzheimer's disease. Aβ(30–40) is in the so-called functional domain required for cytotoxicity and has been shown to adopt a β-strand conformation and to form parallel β sheets.[8] The close relationship between amyloid peptides and HIV fusion peptides has been reported previously.[9]

Based primarily on IR spectroscopic data, the SIVwt peptide has been reported to form aggregated β structures.[10,11] From their analysis of SIVwt peptides with attenuated total reflectance spectroscopy (ATR), Martin et al. reported an IR band typical of β aggregates that contain strong hydrogen bonds.[10] Interestingly, such aggregates have spectroscopic characteristics indistinguishable from those of amyloid fibrils. We noted that samples for the ATR studies were prepared by drying solutions of peptides in dimethyl sulfoxide (DMSO) onto the ATR crystal. Thus, the concentration of the fusion peptide was very high, and little DMSO remained in the sample. However, when dissolved in an aqueous buffer, the retroviral fusion peptides formed large, colloidal aggregates,[10,11] which are spectroscopically identical to those formed in DMSO at low DMSO/peptide molar ratios. Moreover, these aggregates present the same spectroscopic features of the peptide aggregates that form upon peptide-mediated membrane fusion.

The fact that this peptide forms β aggregates in DMSO provides a unique opportunity to study the process of fibril formation in atomic detail with MD simulation techniques.

[*] Prof. X. Daura
Catalan Institution for Research and Advanced Studies (ICREA)
Institute of Biotechnology and Biomedicine
Universitat Autònoma de Barcelona
08193 Bellaterra, Barcelona (Spain)
Fax: (+34) 93-581-2011
E-mail: xavier.daura@uab.es
P. Soto, Prof. A. E. Mark
Groningen Biomolecular Sciences and Biotechnology Institute (GBB)
Department of Biophysical Chemistry, University of Groningen
9747 AG Groningen (The Netherlands)
Prof. J. Cladera
Biophysics Unit
Department of Biochemistry and Molecular Biology
Universitat Autònoma de Barcelona
08193 Bellaterra, Barcelona (Spain)

[**] This work was supported by the Spanish MCyT/FEDER, reference BIO2003-02848. We thank S. Ventura for critical reading of the manuscript.

 DOI: 10.1002/ange.200461935

Owing to its low atom density, DMSO is a much less expensive solvent to simulate than water. This means that it is possible to study the collective properties of large-scale aggregates in explicit solvent.

Figure 1 shows that the parallel β-sheet aggregates spontaneously adopt a helical suprastructure in the simulations. For pb10 (a protofibril construct with 10 parallel chains; see experimental section) the β sheet twists away from the initial planar conformation during the first 20 ns. A dynamic equilibrium is then established involving partial unwinding and rewinding of the suprastructure. The helical twist per chain oscillates between ≈5° and ≈15°. The average twist angle is 10°, and the average helical pitch is 15 nm (calculated for chains 2–7 over the interval of 20–100 ns). Fraying was observed at the ends of the structure, and chains 1, 8, 9, and 10 have less than five hydrogen bonds to their neighbors after 30 ns. Pb20 and pb30 (constructs with 20 and 30 parallel chains, respectively) behave similarly to pb10. The average twist angle and average pitch are 10° and 16 nm for pb20, and 9° and 20 nm for pb30, over the interval of 20–50 ns. As with pb10, only the chains with an average of five interstrand hydrogen bonds or more (7–19 in pb20 and 5–20 in pb30) were included in these estimates. The final structure of pb30 is shown in Figure 2. In all three cases, the ends of the sheet tend to adopt a higher twist angle than the central section. Thus, modeling short fragments would overestimate the degree of twist; indeed, the twists of pb10 and pb20 are slightly greater than that of pb30. In addition, fragments at the ends are found to orient in a different direction to the main axis of the protofilament (helix bending), while still maintaining a helical twist.

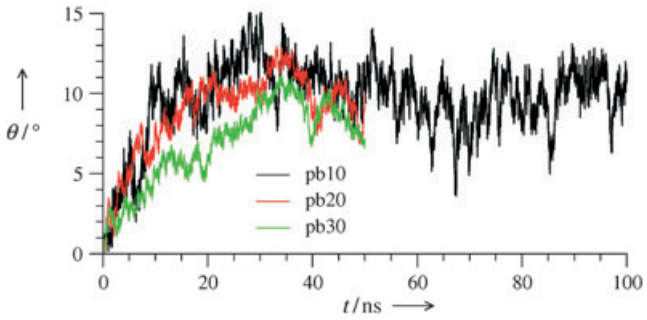

Figure 1. Twist angle per peptide chain in simulations of pb10, pb20, and pb30 as a function of time. The twist angle θ was calculated as $\theta = \arccos(\mathbf{u}_m \cdot \mathbf{u}_n)/(n-m+1)$, in which $\mathbf{u}$ is the unit vector from the α-C atom of residue 1 to that of residue 12 for each chain, and m and n are the first and last chains respectively, in an aggregate with five or more interstrand hydrogen bonds. (These were chains 2–7 in pb10, chains 7–19 in pb20, and chains 5–20 in pb30.)

The supramolecular structure observed in the simulations can be described as a left-handed twisted ribbon with saddlelike curvature.[12] The chirality of the constituent chains renders this structure more thermodynamically stable than a helical ribbon.[2,12] In the simulations, we observed a cooperative twisting of the β sheet until a maximum twist angle was reached. At the point of maximum stress in the geometry, there was a subsequent relaxation toward a smaller angle, followed by alternating partial unwinding/rewinding events around an equilibrium twist angle. The average twist angle of the ribbon, ≈9°, may be compared with twist angles of ≈0.5° to ≈2.5° suggested for multilayered amyloid fibrils,[6,13] with an angle of ≈7° proposed for a speculative model of bilayered β2-microglobulin fibrils,[14] and with twist angles ranging from 0° to ≈30° for single-layer β-sheet motifs in proteins.[15,16]

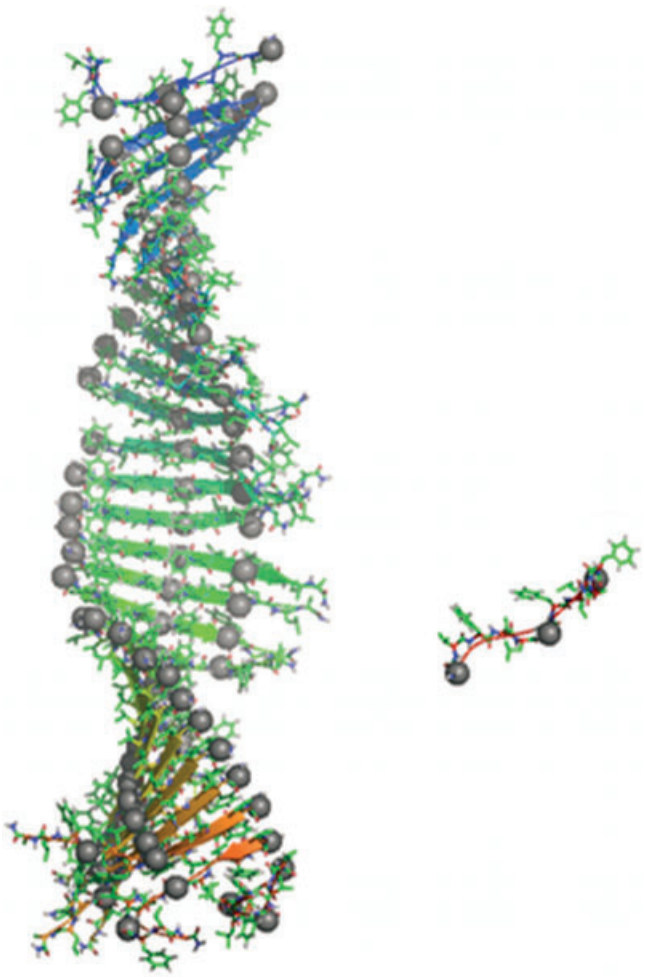

Figure 2. The protofibril pb30 at 50 ns. One terminal chain has dissociated (right). The average twist angle per chain is 9°, and the average pitch (P) is 20 nm at 20–50 ns. The pitch is calculated as $P = N_c \times D_c$, in which N_c is the number of peptide chains per 360° turn and D_c is the translation per chain along the long fibril axis. N_c and D_c are calculated only for intact chains (those bearing at least five or more interstrand hydrogen bonds. See Figure 1).

The cross-β structure of amyloid fibrils inferred from diffraction data (β strands of the precursor polypeptides are perpendicular to, and ribbonlike β sheets are parallel to the fibril axis)[6] is compatible with either a parallel or antiparallel arrangement of the polypeptide strands. Packing depends on the sequence of the polypeptide, and the nature of the interactions between the side chains of neighboring strands. It was recently suggested that an increase of the amphiphilicity of the Aβ(16–22) peptide changes the β sheet structure in the fibrils from antiparallel to parallel.[17] To test the effect of chain orientation on the stability and twisting of the SIVwt

protofibril, a simulation of 10 antiparallel chains in DMSO was performed. A rapid loss of interchain hydrogen bonding was observed (results not shown). After 50 ns, only two adjacent chains had more than five interstrand hydrogen bonds. Therefore, the results suggest that the parallel β sheet arrangement is most stable and that nonpolar interactions between side chains dominate.[18]

We believe that this is the first example in which the spontaneous twisting of a protofibril into an *equilibrium* twisted-ribbon suprastructure has been observed. Recently, Fishwick et al.[19] claimed to have simulated the spontaneous twisting of 20-membered β sheets formed by glutamine-rich peptides with an implicit solvent model. However, the large structural changes observed in the extremely short simulations (100 ps) cast serious doubt on the reliability of the results. In other computational studies of amyloid protofibrils, a specific twist has simply been imposed on the ribbon structure with simulations serving only to relax the initial conformation.[20] Our work demonstrates that it is possible to model stable protofibril structures at an atomic level. Studies of the spontaneous aggregation of this peptide into extended β sheet structures are under way.

Experimental Section

Four systems were simulated. Three were β-sheet constructs containing 10 (pb10), 20 (pb20), and 30 (pb30) parallel SIVwt chains. The construct pb10 was simulated for 100 ns, pb20 and pb30 for 50 ns. The initial arrangement of the β sheets was planar. The average distance between facing α-C atoms was 0.4 nm. The long axis of the β sheet was ~4 nm for pb10, ~8 nm for pb20, and ~12 nm for pb30. Each β sheet was placed in a periodic cuboid of $8 \times (D+4) \times 7\ nm^3$ (D = length of the long axis) and solvated with DMSO.[21] A fourth system consisting of 10 peptide chains in an antiparallel arrangement (ab10) was also simulated to test the effect of the orientation of the peptide on the stability of the protofibril. All simulations were performed with the GROMACS software[22] and the GROMOS 43 A1 force field.[23] The end groups of the peptide were neutral (H_2N–, –$CONH_2$) in accordance with experimental data. The temperature and pressure were coupled to external baths[24] at 300 K and 1 bar with relaxation times of 0.1 and 0.5 ps, respectively. Bond lengths were constrained with the LINCS algorithm.[25] The equations of motion were integrated with the leap-frog algorithm with a time step of 2 fs. Nonbonding interactions were evaluated with a twin-range cutoff of 0.8/1.4 nm, and a charge-group pair list updated every 10 time steps.

Received: September 9, 2004
Published online: January 3, 2005

Keywords: aggregation · molecular dynamics · peptides · protein models · protofibrils

[1] R. Tycko, *Curr. Opin. Chem. Biol.* **2000**, *4*, 500.
[2] S. Zhang, D. M. Marini, W. Hwang, S. Santoso, *Curr. Opin. Chem. Biol.* **2002**, *6*, 865.
[3] C. M. Dobson, *Philos. Trans. R. Soc. London Ser. B* **2001**, *356*, 133.
[4] M. Sunde, C. C. Blake, *Q. Rev. Biophys.* **1998**, *31*, 1.
[5] A. T. Petkova, Y. Ishii, J. J. Balbach, O. N. Antzutkin, R. D. Leapman, F. Delaglio, R. Tycko, *Proc. Natl. Acad. Sci. USA* **2002**, *99*, 16742.
[6] J. L. Jiménez, E. J. Nettleton, M. Bouchard, C. V. Robinson, C. M. Dobson, H. R. Saibil, *Proc. Natl. Acad. Sci. USA* **2002**, *99*, 9196.
[7] M. Horth, B. Lambrecht, M. C. L. Khim, F. Bex, C. Thiriart, J. M. Ruysschaert, A. Burny, R. Brasseur, *EMBO J.* **1991**, *10*, 2747.
[8] O. N. Antzutkin, J. J. Balbach, R. D. Leapman, N. W. Rizzo, J. Reed, R. Tycko, *Proc. Natl. Acad. Sci. USA* **2000**, *97*, 13045.
[9] a) T. Pillot, M. Goethals, B. Vanloo, C. Talussot, R. Brasseur, J. Vandekerckhove, M. Rosseneu, L. Lins, *J. Biol. Chem.* **1996**, *271*, 28757; b) W. M. Wojtowicz, M. Farzan, J. L. Joyal, K. Carter, G. J. Babcock, D. I. Israel, J. Sodroski, T. Mirzabekov, *J. Biol. Chem.* **2002**, *277*, 35019; c) A. Saez-Cirion, J. L. Nieva, W. R. Gallaher, *AIDS Res. Hum. Retroviruses* **2003**, *19*, 969; d) L. M. Gordon, P. W. Mobley, W. Lee, S. Eskandari, Y. N. Kaznessis, M. A. Sherman, A. J. Waring, *Protein Sci.* **2004**, *13*, 1012.
[10] I. Martin, M. C. Dubois, F. Defrise-Quertain, T. Saermark, A. Burny, R. Brasseur, J. M. Ruysschaert, *J. Virol.* **1994**, *68*, 1139.
[11] a) J. Cladera, I. Martin, J. M. Ruysschaert, P. O'Shea, *J. Biol. Chem.* **1999**, *274*, 29951; b) J. L. Nieva, S. Nir, A. Muga, F. M. Goñi, J. Wilschut, *Biochemistry* **1994**, *33*, 3201.
[12] R. Oda, I. Huc, M. Schmutz, S. J. Candau, F. C. MacKintosh, *Nature* **1999**, *399*, 566.
[13] a) K. Lu, J. Jacob, P. Thiyagarajan, V. P. Conticello, D. G. Lynn, *J. Am. Chem. Soc.* **2003**, *125*, 6391; b) T. S. Burkoth, T. L. S. Benzinger, V. Urban, D. M. Morgan, D. M. Gregory, P. Thiyagarajan, R. E. Botto, S. C. Meredith, D. G. Lynn, *J. Am. Chem. Soc.* **2000**, *122*, 7883.
[14] M. I. Ivanova, M. R. Sawaya, M. Gingery, A. Attinger, D. Eisenberg, *Proc. Natl. Acad. Sci. USA* **2004**, *101*, 10584.
[15] C. Chothia, T. Hubard, S. Brenner, H. Barns, A. Murzin, *Annu. Rev. Biophys. Biomol. Struct.* **1997**, *26*, 597.
[16] For a more in-depth review on fibril morphologies, see: L. C. Serpell, *Biochim. Biophys. Acta* **2000**, *1502*, 16.
[17] D. J. Gordon, J. J. Balbach, R. Tycko, S. C. Meredith, *Biophys. J.* **2004**, *86*, 428.
[18] a) S. Ventura, E. Lacroix, L. Serrano, *J. Mol. Biol.* **2002**, *322*, 1147; b) M. López de la Paz, K. Goldie, J. Zurdo, E. Lacroix, C. M. Dobson, A. Hoenger, L. Serrano, *Proc. Natl. Acad. Sci. USA* **2002**, *99*, 16052; c) S. Ventura, J. Zurdo, S. Narayanan, M. Parreno, R. Mangues, B. Reif, F. Chiti, E. Giannoni, C. M. Dobson, F. X. Aviles, L. Serrano, *Proc. Natl. Acad. Sci. USA* **2004**, *101*, 7258.
[19] C. W. G. Fishwick, A. J. Beevers, L. M. Carrick, C. D. Whitehouse, A. Aggeli, N. Boden, *Nano Lett.* **2003**, *3*, 1475.
[20] a) L. Li, T. A. Darden, L. Bartolotti, D. Kominos, L. G. Pedersen, *Biophys. J.* **1999**, *76*, 2871; b) W. M. Hwang, D. M. Marini, R. D. Kamm, S. Q. Zhang, *J. Chem. Phys.* **2003**, *118*, 389.
[21] H. Liu, F. Müller-Plathe, W. F. van Gunsteren, *J. Am. Chem. Soc.* **1995**, *117*, 4363.
[22] a) H. J. C. Berendsen, D. van der Spoel, R. van Drunen, *Comput. Phys. Commun.* **1995**, *91*, 43; b) E. Lindahl, B. Hess, D. van der Spoel, *J. Mol. Model.* **2001**, *7*, 306.
[23] a) X. Daura, A. E. Mark, W. F. van Gunsteren, *J. Comput. Chem.* **1998**, *19*, 535; b) W. F. van Gunsteren, S. R. Billeter, A. A. Eising, P. H. Hünenberger, P. Krüger, A. E. Mark, W. R. P. Scott, I. G. Tironi, *Biomolecular Simulation: The GROMOS96 Manual and User Guide*, vdf Hochschulverlag AG an der ETH, Zürich, and BIOMOS BV, Groningen, **1996**.
[24] H. J. C. Berendsen, J. P. M. Postma, W. F. van Gunsteren, A. DiNola, J. R. Haak, *J. Chem. Phys.* **1984**, *81*, 3684.
[25] B. Hess, H. Bekker, H. J. C. Berendsen, J. G. E. M. Fraaije, *J. Comput. Chem.* **1997**, *18*, 1463.

